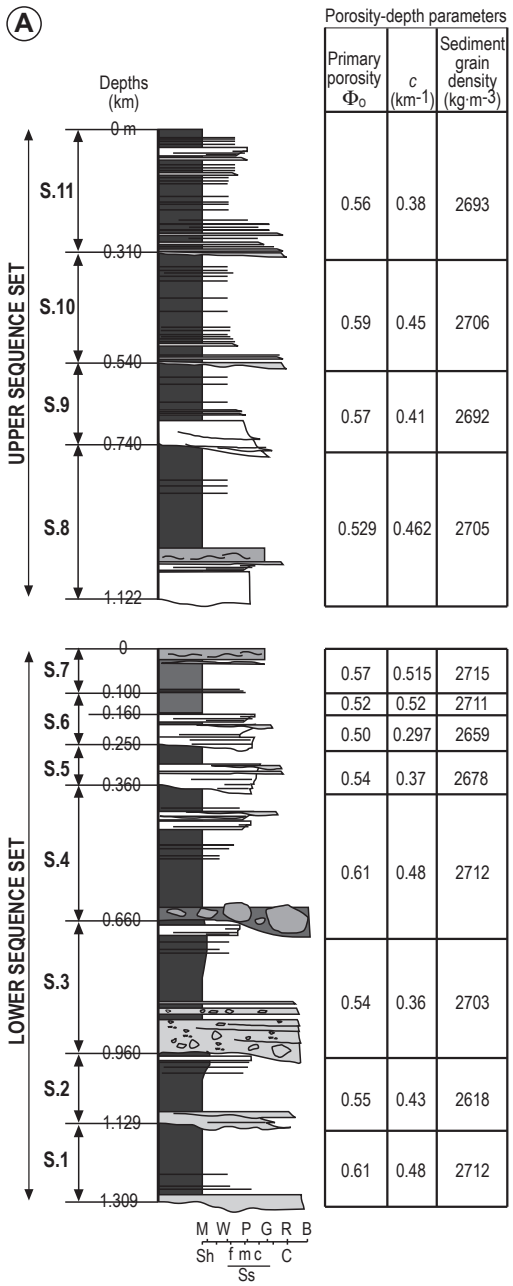

LITHOLOGY	POROSITY DEPTH PARAMETERS		
	Surface porosity Φ_o	c (km^{-1})	Sediment grain density ($kg \cdot m^{-3}$)
	(2)	(3)	(1)
Limestone (mudstone)	0.51	0.52	2710
Shale and marlstone	0.63	0.51	2720
Siltstone	0.56	0.39	2680
Sandstone	0.49	0.27	2650
Conglomerate	0.50	0.3	2600
Calcareous breccia	0.50	0.3	2700

(1) Allen & Allen (1990)
(2) Magara (1980), Bond & Kominz (1984), Stam *et al*. (1987) and Vergés *et al*. (1998)
(3) Sclater & Christie (1980), Schmoker & Halley (1982) and Vergés *et al*. (1998)

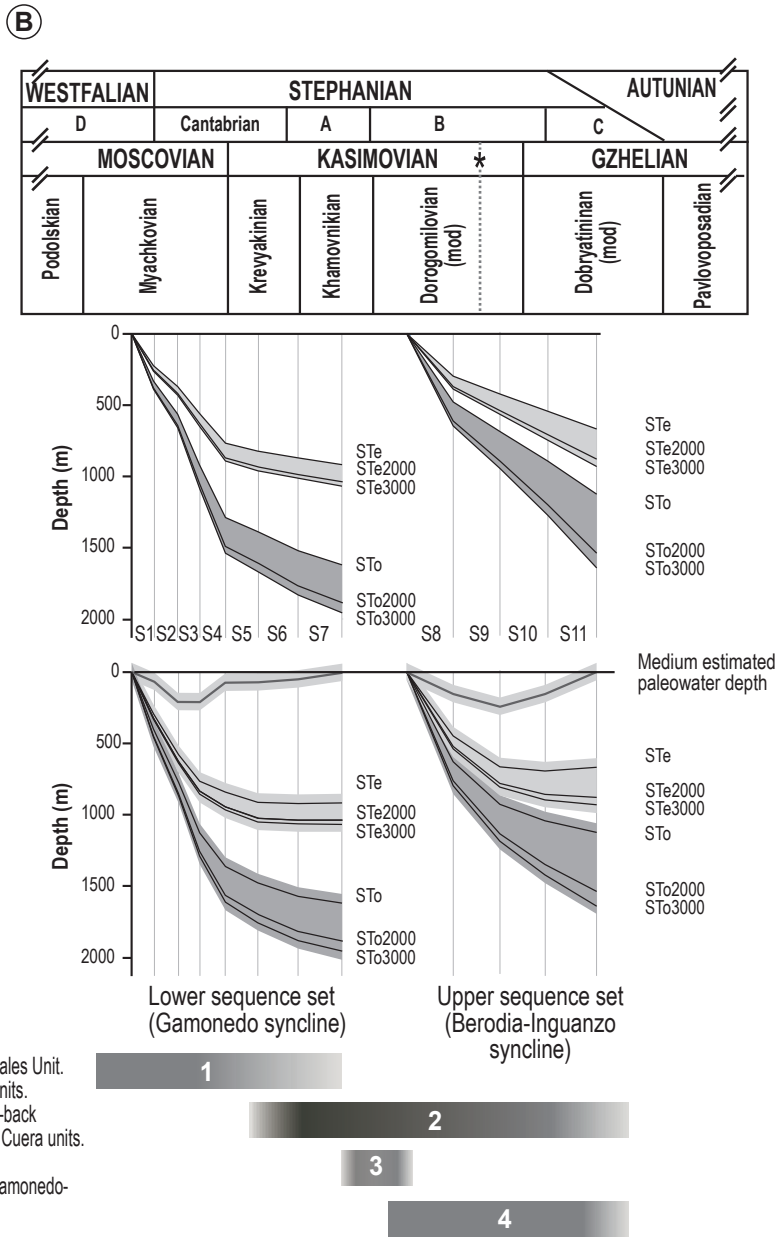

1) Emplacement of the Cuera and the Gamonedo-Cabrales Unit. First phase of thrusting in the Gamonedo-Cabrales units.
2) Emplacement of the Central and Frontal units. Piggy-back southward transport of the Gamonedo-Cabrales and Cuera units.
3) Tectonic unplift
4) Second phase of thrusting (out of sequence) in the Gamonedo-Cabrales Unit.

Merino-Tomé et al. Data repository. Figure 1

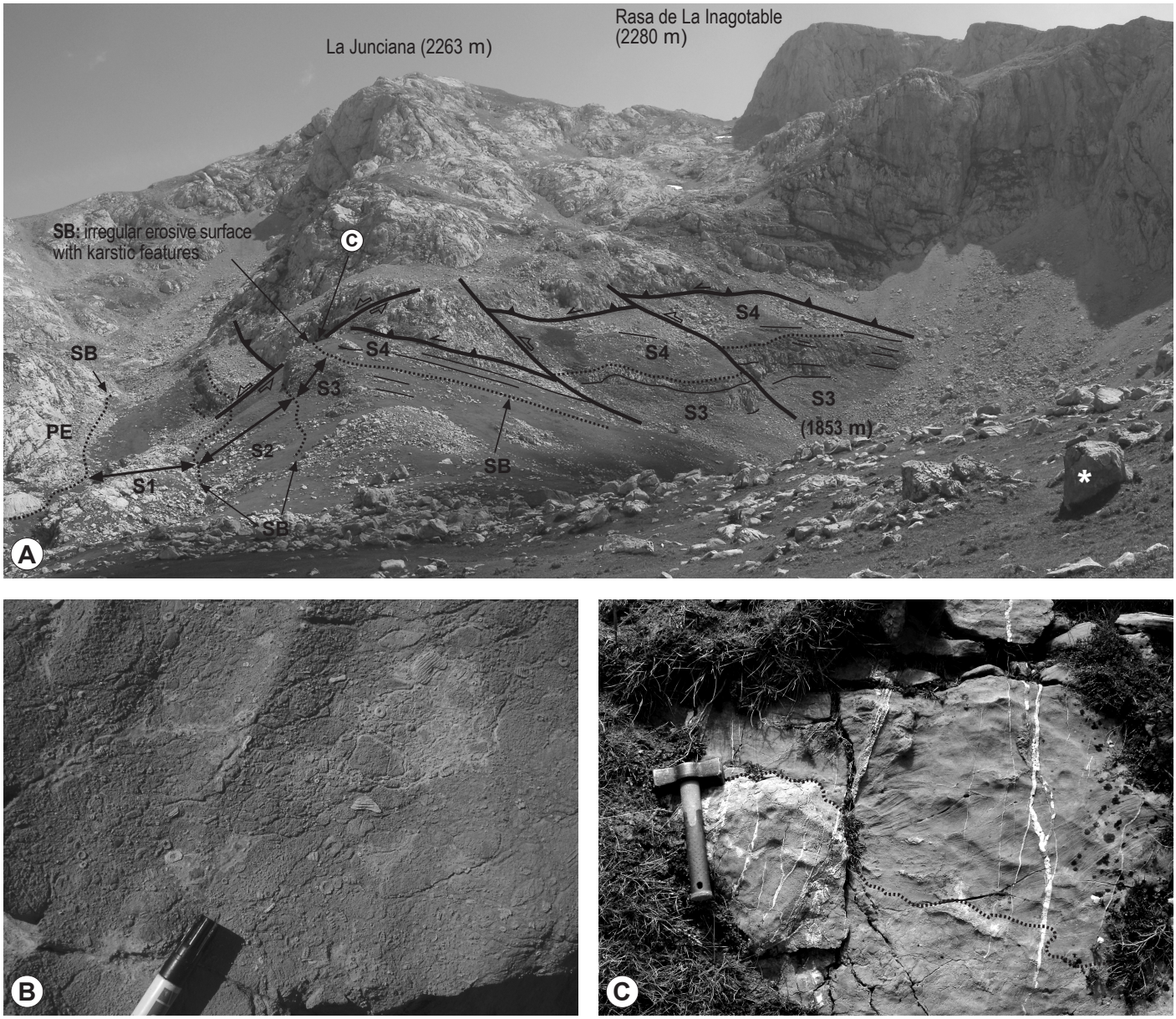

Merino-Tomé et al. Data Repository. Figure 2

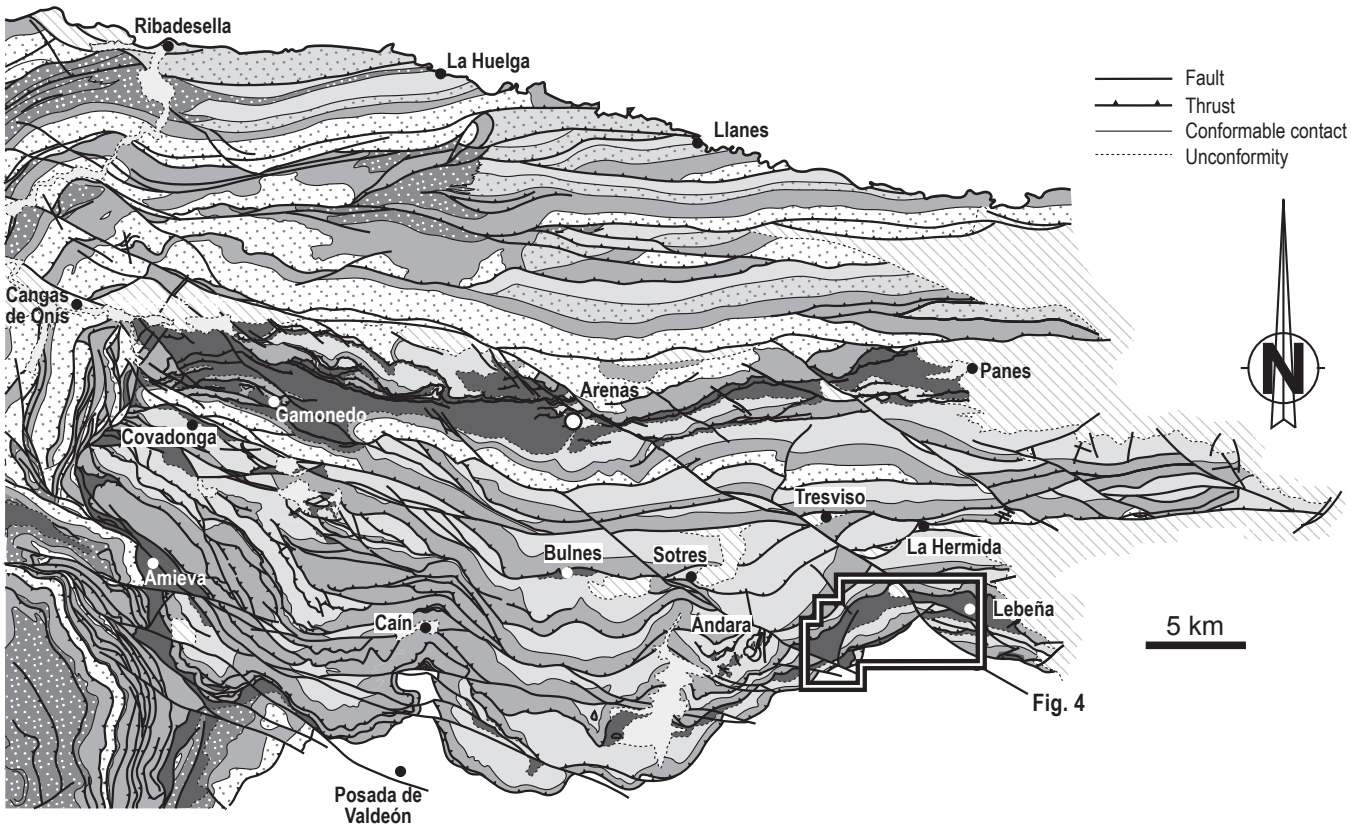

Merino-Tomé et al. Data Repository. Figure 03

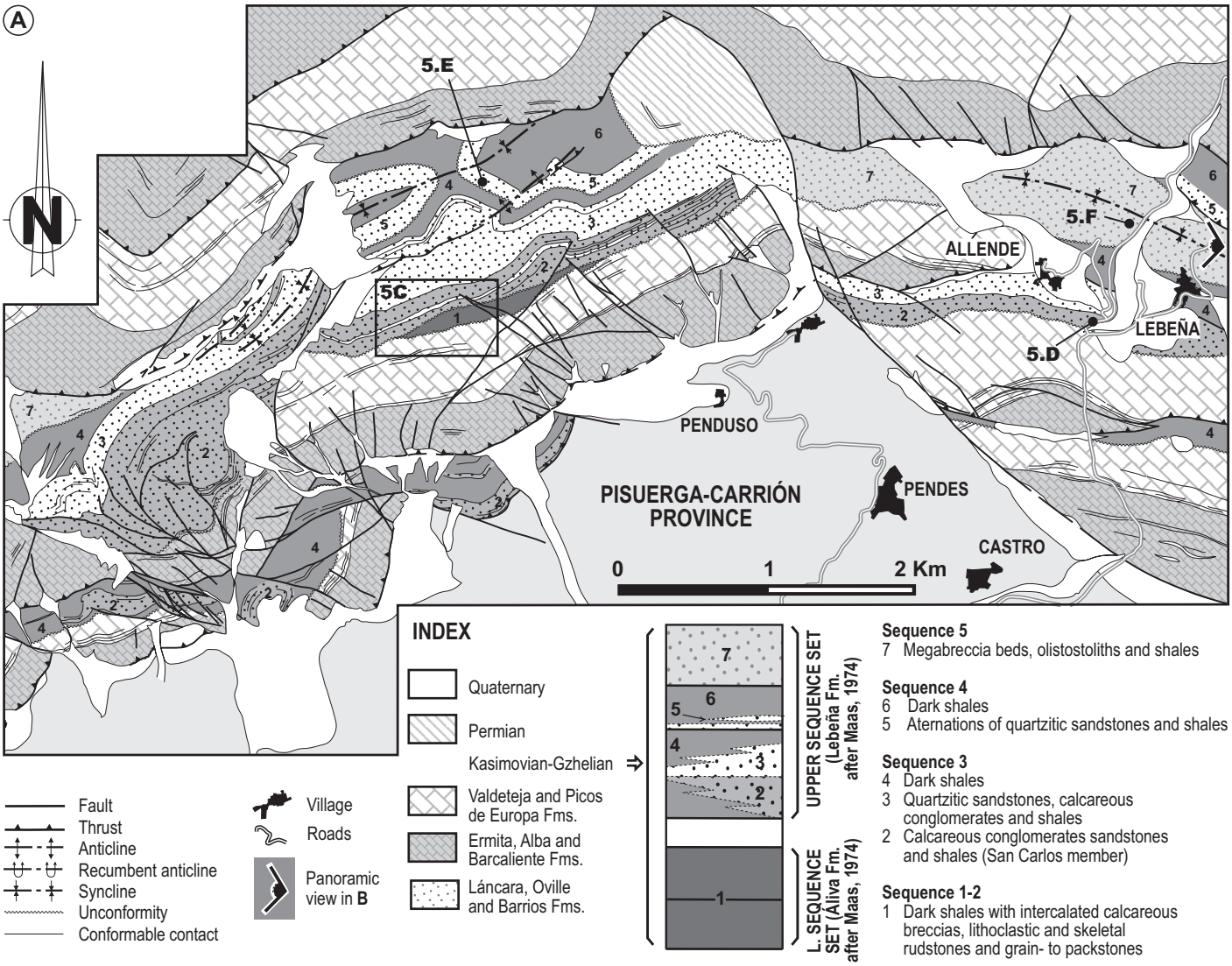

Merino-Tomé et al. Data Repository. Figure 4

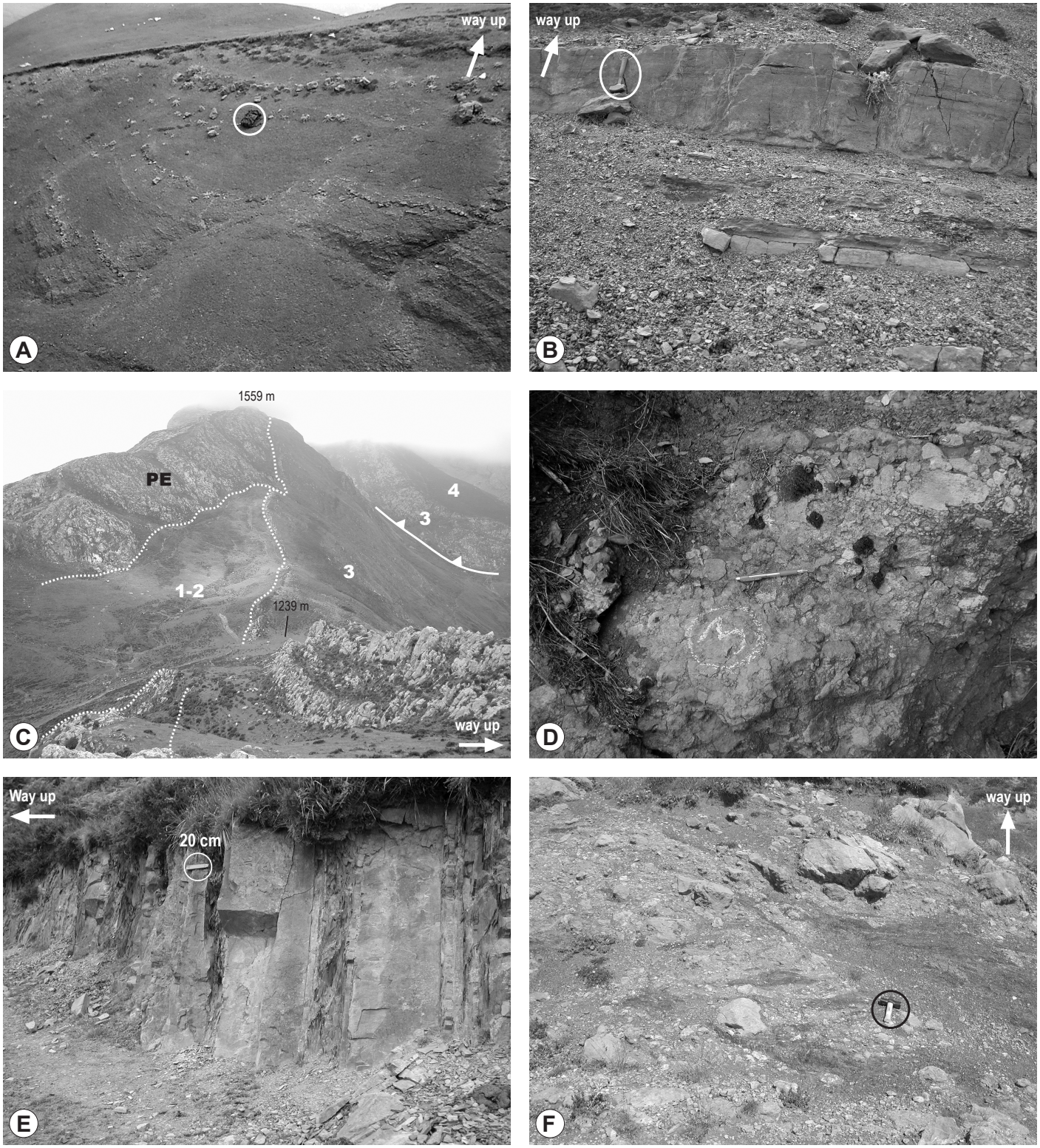

Merino-Tomé et al. Data Repository. Figure 5

DATA REPOSITORY

FIGURE CAPTIONS

Figure DR1. Subsidence curves for the lower sequence set in the Gamonedo syncline and for the upper sequence set in the Berodia-Inguanzo syncline (Modified after Merino-Tomé et al., 2007). **A**) Composite stratigraphic sections used for the analysis. The medium porosity depth parameters estimated on the basis of the values for single lithologies are also shown. **B**) Tectonic subsidence (STe) and total subsidence (STo) curves with added loads of 2000 and 3000 m of sediment (STe+2000 and STe+3000; STo+2000 and STo+3000) to accomplish the sedimentary loads removed by erosion (a minimum of 1000 m of sediments existed below the base of the Permo-Mesozoic succession in both Gamonedo and Berodia synclines considering the mean dip of the Cretaceous in the nearby outcrops). Palaeobathymetric curves (Cbat), STe+Cbat and STo+Cbat are the result of combining palaeobathymetric and tectonic or total subsidence curves, respectively. An error margin of 100 m is assumed for the paleobathymetric estimations.

Figure DR2. Syntectonic strata in the Vegas de Ándara area (SE part of the Central Unit, see Fig. 2 for location). **A**) Panoramic view of the Vegas de Ándara in which the 4 depositional sequences that form the syntectonic succession in this area can be recognized (S1-S4). **B**) Clast-supported calcareous breccias from sequence 1 containing abundant skeletal grains. The width of the marker used as a scale is 16 mm. **C**) Irregular erosive unconformity at the base of sequence 4 (black dashed line). The underlying limestones are pervasively brecciated and show clear evidence of subaerial exposure and karstification. Overlying lithic sandstones display trough cross bedding and correspond to littoral fan-delta front and fluviatile sediments. The hammer for scale is 25 cm long.

Figure DR3. Synthetic geological map of the Eastern part of the Ponga Nappe Province and Picos de Europa Province showing the location of the geological map depicted in Fig. DR3.A.

Figure DR4. A) Detailed geological map of the easternmost part of the Frontal Unit (see Fig. DR3 for location) showing the distribution of the Kasimovian-Gzhelian syntectonic strata and their relationships with the underlying Carboniferous pre-tectonic strata. B) Panoramic view of the Lebeña Valley. The main stratigraphic units and tectonic structures are indicated (B,V,PE, Barcaliente, Valdeteja and Picos de Europa Formations; numbers refers to the legend in Fig. DR4.A). Note the large limestone blocks (*) included in large-scale megabreccia units characterizing sequence 5. These deposits serve to time the T1 thrust.

Figure DR5. Syntectonic successions in the Frontal Unit. A) Dark shales with thin intercalations of detrital limestones of the Áliva Formation at Vegas de Áliva (sequence 2). Encircled a 70-cm long back-pack. B) Calcareous detrital beds within the Áliva Formation (sequence 2). Calcareus detrital components mostly include Picos de Europa and early-mid Kasimovian lithoclasts and skeletal grains. Detrital quartz grains are present but only in small amounts, and quartzitic pebbles, although the can be found locally, are rare. 25-cm-long hammer for scale (encircled). C) Panoramic view showing the unconformities at the base of the lower sequence set (sequences 1 and 2) and upper sequence set (San Carlos conglomerates, sequence 3) in the vicinity of Penduso (see Fig. DR4.A for location). D) Detail of a conglomerate bed at the base of the Lebeña Formation (see Fig DR4 for location). The pencil used for scale is 14 cm long. E) Quartzitic and sublitharenitic sandstone beds of the lower part of sequence 4 accumulated by sand-laden hiperpycnal flows generated during high river discharges in fan deltas located on the S boundary of the Central Unit. F) Thick

debris flow deposits of sequence 5. Large lithified fragments of the calcareous detrital deposits of sequences 1 and 2 are commonly found in these deposits. Harmer for scale is 25 cm long.

REFERENCES

Allen, P.A. and Allen, J.R., 1990, Basin Analysis: Principles and Applications: Oxford, Blackwell Scientific Publications, 451 pp.

Bond, G.C. and Kominz, M.A., 1984, Construction of tectonic subsidence curves for the Early Paleozoic miogeocline, southern Canadian Rocky Mountains: implications for subsidence mechanisms, age of breakup, and crustal thinning. Geological Society of America Bulletin, v. 95, p. 155-173.

Magara, K., 1980, Comparison of porosity-depth relationships of shale and sandstone. Journal of Petroleoum Geology, v. 3, p. 175-185.

Schmoker, J.G. and Halley, R.B., 1982, Carbonate porosity versus depth: a predictable relation for South Florida. American Association of Petroleum Geologists Bulletin, v. 66, p. 2561-2570.

Sclater, J.G. and Christie, P.A.F., 1980, Continental stretching: an explanation of the post-mid-Cretaceous subsidence of the Central North Sea Basin. Journal of Geophyscal Research, v. 85, p. 3711-3739.

Stam, B., Gradstein, F.M., Lloyd, P. and Gillis, D., 1987, Algorithms for porosity and subsidence history. Computer Geosciences, v. 13, p. 317-349.

Vergés, J., Marzo, M., Santaeularia, T., Serra-Kiel, J., Burbank, D.W., Muñoz, J.A., and Giménez-Montsant, J., 1998, Quantified vertical motions and tectonic evolution of the SE Pyrenean foreland basin, *in* Mascle, A., et al., eds., Cenozoic Foreland

Basins of Western Europe: London, Geological Society, Special Publication, v. 134, p. 107-134.